

Electroexcitation of the Roper resonance from CLAS data

Inna Aznauryan^{1,2} and Volker Burkert¹

¹ Thomas Jefferson National Accelerator Facility, Newport News, Virginia 23606, USA

² Yerevan Physics Institute, 375036 Yerevan, Armenia

October 27, 2007

Abstract. The helicity amplitudes of the electroexcitation of the Roper resonance on proton are extracted at $1.7 < Q^2 < 4.2 \text{ GeV}^2$ from recent high precision JLab-CLAS cross sections data and longitudinally polarized beam asymmetry for π^+ electroproduction on protons. The analysis is made using two approaches, dispersion relations and unitary isobar model, which give consistent results. It is found that the transverse helicity amplitude for the $\gamma^*p \rightarrow P_{11}(1440)$ transition, which is large and negative at $Q^2 = 0$, becomes large and positive at $Q^2 \simeq 2 \text{ GeV}^2$, and then drops slowly with Q^2 . Longitudinal helicity amplitude, that was previously found from CLAS data as large and positive at $Q^2 = 0.4, 0.65 \text{ GeV}^2$, drops with Q^2 . These results rule out the presentation of $P_{11}(1440)$ as a q^3G hybrid state, and provide strong evidence in favor of this resonance as a first radial excitation of the $3q$ ground state.

PACS. 1.55.Fv, 13.60.Le, 13.40.Gp, 14.20.Gk

In this talk we report our results on the electroexcitation of the Roper resonance ($P_{11}(1440)$) extracted from a large body of CLAS data on differential cross sections and polarized beam asymmetries for the process $ep \rightarrow en\pi^+$ in the range of invariant hadronic mass $W = 1.15 - 1.69 \text{ GeV}$ and photon virtuality $Q^2 = 1.7 - 4.2 \text{ GeV}^2$ with full azimuthal and polar angle coverage [1]. Combined with the information obtained from the previous CLAS data at $Q^2 = 0.4, 0.65 \text{ GeV}^2$ [2,3] and that at $Q^2 = 0$ [4], these results give us knowledge of the Roper electroexcitation in wide Q^2 range and allow us to draw quite definite conclusions on the nature of $P_{11}(1440)$.

It is known that the structure of the Roper resonance has attracted special attention since its discovery, because the simplest and most natural assumption that this is a first radial excitation of the $3q$ ground state led to the difficulties in the description of the resonance. To deal with shortcomings of the quark model, alternative, as well extended descriptions of $P_{11}(1440)$ were developed: as a hybrid (q^3G) state [5,6], that of a quark core dressed by a meson cloud [7,8], a dynamically generated πN resonance [9], and presentations that include $3q - q\bar{q}$ components, in particular, strong σN component (see Ref. [10] and references therein).

The Q^2 dependence of the electromagnetic transition form factors is highly sensitive to different descriptions of the Roper state. However, until recently, the data base needed to measure these form factors at relatively high Q^2 was almost exclusively based on π^0 production, and was very limited in kinematical coverage. Also, the $\pi^0 p$ final state is dominated by the nearby isospin $3/2$ $\Delta(1232)$ resonance, whereas the isospin $1/2$ Roper state couples

more strongly to the $\pi^+ n$ channel. The data [1] allow us to extract the $\gamma^*p \rightarrow P_{11}(1440)$ helicity amplitudes at $Q^2 = 1.7 - 4.2 \text{ GeV}^2$, and therefore to obtain complete picture of the electroexcitation of the Roper resonance in a wide Q^2 region.

The approaches we use are fixed- t dispersion relations (DR) and unitary isobar model (UIM), which both were successfully employed in Refs. [2,3,11] to analyze photo-production and low Q^2 electroproduction of pions. These approaches were presented and discussed in Refs. [11].

The imaginary parts of the amplitudes in both approaches are determined mainly by s -channel resonance contributions which we parameterize in the Breit-Wigner form with energy-dependent widths [11,12]. The exception was made for the $P_{33}(1232)$ resonance which was treated in a special way. According to the phase-shift analyses of the πN scattering, the πN amplitude corresponding to the $P_{33}(1232)$ resonance is elastic up to $W = 1.43 \text{ GeV}$ (see, for example, the latest GWU(VPI) analyses [13,14]). In combination with DR and Watson's theorem, this provides strict constraints on the multipole amplitudes $M_{1+}^{3/2}$, $E_{1+}^{3/2}$, $S_{1+}^{3/2}$ that correspond to the $P_{33}(1232)$ resonance. In particular, as it was shown in Ref. [11], the shape of $M_{1+}^{3/2}$ is close to that at $Q^2 = 0$ from the GWU(VPI) analysis [15]. This constraint on the large $M_{1+}^{3/2}$ amplitude plays an important role in the reliable extraction of the $P_{11}(1440)$ electroexcitation amplitudes, because the $P_{33}(1232)$ and $P_{11}(1440)$ states are strongly overlapping.

We have taken into account all resonances from the first, second, and third resonance regions. These are 4- and 3-star resonances $P_{33}(1232)$, $P_{11}(1440)$, $D_{13}(1520)$,

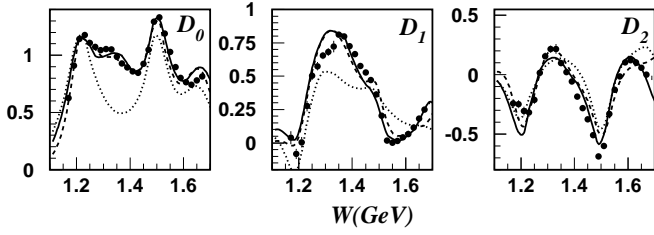


Fig. 1. Experimental data for the Legendre moments of the structure function $\sigma_T + \epsilon\sigma_L$ at $Q^2 = 2.05 \text{ GeV}^2$ [1] in comparison with our results; the units are $\mu\text{b/sr}$. Solid and dashed curves correspond to the DR and UIM results, respectively. Dotted curves are obtained by switching off the $P_{11}(1440)$ resonance from the DR results.

$S_{11}(1535)$, $P_{33}(1600)$, $S_{31}(1620)$, $S_{11}(1650)$, $D_{15}(1675)$, $F_{15}(1680)$, $D_{13}(1700)$, $D_{33}(1700)$, $P_{11}(1710)$, and $P_{13}(1720)$. The masses, widths, and πN branching ratios of these resonances were taken equal to the mean values of the data presented in the Review of Particle Physics (RPP) [4]. At each Q^2 , we have made two kinds of fits in both approaches: (i) The magnitudes of the helicity amplitudes corresponding to all resonances listened above were fitted. (ii) The transverse amplitudes for the members of the multiplet $[70, 1^-]$: $S_{31}(1620)$, $S_{11}(1650)$, $D_{15}(1675)$, $D_{13}(1700)$, and $D_{33}(1700)$, were fixed according to the single quark transition model [16], which relates these amplitudes to those for $D_{13}(1520)$ and $S_{11}(1535)$; the longitudinal amplitudes of these resonances and the amplitudes of the resonances $P_{33}(1600)$, $P_{11}(1710)$, and $P_{13}(1720)$ were taken equal to 0. It turned out that the results obtained for $P_{33}(1232)$, $P_{11}(1440)$, $D_{13}(1520)$, and $S_{11}(1535)$ in the two fits are close to each other. The amplitudes of the Roper resonance presented below are the average values of the results obtained in these fits.

In Fig. 1, we present the comparison of our results with the experimental data for the Legendre moments of the structure function $\sigma_T + \epsilon\sigma_L$ at $Q^2 = 2.05 \text{ GeV}^2$ [1]. The Legendre moment $D_0^{T+\epsilon L}$ does not contain interference of different multipole amplitudes and is related to the sum of squares of these amplitudes. The resonance behavior of the multipole amplitudes is revealed in $D_0^{T+\epsilon L}$ in the form of enhancements. Resonance structures related to the narrow resonances $P_{33}(1232)$, $D_{13}(1520)$, and $S_{11}(1535)$ are clearly seen in $D_0^{T+\epsilon L}$. There is a shoulder between the Δ and 1.5 GeV peaks, which is related to the broad Roper resonance. To demonstrate this we present in Fig. 1 by dotted curves the results obtained by switching off the $P_{11}(1440)$ resonance from the DR results. To stress the advantage of the investigation of the Roper resonance in the reaction $\gamma^*p \rightarrow \pi^+n$, we note that for this reaction, the relative contribution of $P_{11}(1440)$ in comparison with $P_{33}(1232)$ in $D_0^{T+\epsilon L}$ is 4 times larger than for $\gamma^*p \rightarrow \pi^0p$.

We now discuss the results for the $\gamma^*p \rightarrow P_{11}(1440)$ helicity amplitudes presented in Table 1 and Fig. 2.

It can be seen that the results obtained using DR and UIM are close to each other. As the non-resonant backgrounds of these approaches are built in conceptually dif-

$Q^2 \text{ (GeV}^2\text{)}$	$A_{1/2}$	$S_{1/2}$
	DR	
1.72	$72.5 \pm 1.0 \pm 4.3$	$24.8 \pm 1.4 \pm 5.3$
2.05	$72.0 \pm 0.9 \pm 4.2$	$21.0 \pm 1.7 \pm 5.0$
2.44	$50.0 \pm 1.0 \pm 3.2$	$9.3 \pm 1.3 \pm 4.1$
2.91	$37.5 \pm 1.1 \pm 2.8$	$9.8 \pm 2.0 \pm 2.3$
3.48	$29.6 \pm 0.8 \pm 2.7$	$4.2 \pm 2.5 \pm 2.3$
4.16	$19.3 \pm 2.0 \pm 3.9$	$10.8 \pm 2.8 \pm 4.5$
$Q^2 \text{ (GeV}^2\text{)}$	UIM	
	$A_{1/2}$	$S_{1/2}$
1.72	$58.5 \pm 1.1 \pm 4.2$	$26.9 \pm 1.3 \pm 5.3$
2.05	$62.9 \pm 0.9 \pm 3.3$	$15.5 \pm 1.5 \pm 4.9$
2.44	$56.2 \pm 0.9 \pm 3.2$	$11.8 \pm 1.4 \pm 4.1$
2.91	$42.5 \pm 1.1 \pm 2.8$	$13.8 \pm 2.1 \pm 2.3$
3.48	$32.6 \pm 0.9 \pm 2.6$	$14.1 \pm 2.4 \pm 2.0$
4.16	$23.1 \pm 2.2 \pm 4.8$	$17.5 \pm 2.6 \pm 5.5$

Table 1. The $\gamma^*p \rightarrow P_{11}(1440)$ helicity amplitudes (in $10^{-3} \text{ GeV}^{-1/2}$ units) found from the analysis of π^+ electroproduction data [1] using DR and UIM. First uncertainty has statistical nature, it was obtained in the fitting procedure. Second uncertainty is systematic one; it is connected with the averaging procedure of the results obtained in two kinds of fits, discussed in the text, and with the uncertainties of the background caused by the uncertainties of the nucleon, pion and $\rho(\omega) \rightarrow \pi\gamma$ form factors.

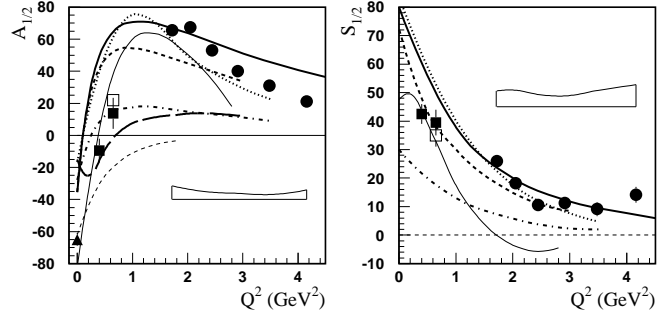


Fig. 2. Helicity amplitudes for the $\gamma^*p \rightarrow P_{11}(1440)$ transition (in $10^{-3} \text{ GeV}^{-1/2}$ units). Full circles are the average values of our results obtained from the analysis of π^+ electroproduction data [1] using DR and UIM. The bands present the systematic uncertainties which are caused by the averaging procedure and by systematic uncertainties mentioned in the caption to Table 1. Full boxes are the results obtained from CLAS data [2, 17, 18, 19, 20]; open boxes present the results of the combined analysis of CLAS single π and 2π electroproduction data [3]. Full triangle at $Q^2 = 0$ is the RPP estimate [4]. Thick curves correspond to the light-front relativistic quark models: dotted, dashed, dash-dotted, long-dashed, and solid curves are from Refs. [21, 22, 23, 24, 25], respectively. Thin solid curves are the predictions obtained for the Roper resonance treated as a quark core dressed by a meson cloud [7, 8]. Thin dashed curves are obtained assuming that $P_{11}(1440)$ is a q^3G hybrid state [6].

ferent ways, we conclude that the model uncertainties of the obtained results are small.

Combined with the information obtained from the previous CLAS data at $Q^2 = 0.4, 0.65 \text{ GeV}^2$ [2, 3, 17, 18, 19, 20], and that at $Q^2 = 0$ [4], new results show nontrivial behavior of the transverse helicity amplitude $A_{1/2}$: being

large and negative at $Q^2 = 0$, it crosses zero between $Q^2 = 0.4$ and 0.65 GeV^2 and becomes large and positive at $Q^2 \simeq 2 \text{ GeV}^2$. Further with increasing Q^2 , this amplitude drops smoothly in magnitude. The longitudinal helicity amplitude $S_{1/2}$, which is large and positive at small Q^2 , drops smoothly with increasing Q^2 .

In Fig. 2, we compare our results with model predictions. These are (i) quark model predictions [21, 22, 23, 24, 25] where the $P_{11}(1440)$ is described as the first radial excitation of the $3q$ ground state; (ii) those assuming the $P_{11}(1440)$ is a hybrid state [6]; and (iii) the results for the Roper resonance treated as a quark core (which is a radial excitation of the $3q$ ground state) dressed by a meson cloud [7, 8].

It is known that with increasing Q^2 , when the momentum transfer becomes larger than the masses of the constituent quarks, a relativistic treatment of the electroexcitation of the nucleon resonances, which is important already at $Q^2 = 0$, becomes crucial. The consistent way to realize the relativistic treatment of the $\gamma^* N \rightarrow N^*$ transitions is to consider them in the LF dynamics. In Fig. 2 we compare our results with the predictions of the LF quark models [21, 22, 23, 24, 25].

All LF approaches [21, 22, 23, 24, 25] give good description of the nucleon form factors, however, the predictions for the $\gamma^* N \rightarrow P_{11}(1440)$ helicity amplitudes are quite different. This is caused by the large sensitivity of these amplitudes to the N and $P_{11}(1440)$ wave functions [25].

The approaches [21, 22, 23, 24, 25] fail to describe the value of the transverse amplitude $A_{1/2}$ at $Q^2 = 0$. This can be an indication of a large meson cloud contribution to the $\gamma^* p \rightarrow P_{11}(1440)$ which is expected to be significant at small Q^2 . As a confirmation of this assumption one can consider the results of Refs. [7, 8] where this contribution is taken into account, and a good description of the helicity amplitudes is obtained at small Q^2 .

In spite of differences, all LF predictions for the $\gamma^* p \rightarrow P_{11}(1440)$ helicity amplitudes have common features which agree with the results extracted from the experimental data: (i) the sign of the transverse amplitude $A_{1/2}$ at $Q^2 = 0$ is negative, (ii) the sign of the longitudinal amplitude $S_{1/2}$ is positive, (iii) all LF approaches predict the sign change of the transverse amplitude $A_{1/2}$ at small Q^2 . We take this qualitative agreement as the evidence in the favor of the $P_{11}(1440)$ resonance as a radial excitation of the $3q$ ground state. Final confirmation of this conclusion requires complete simultaneous description of the nucleon form factors and the $\gamma^* p \rightarrow P_{11}(1440)$ amplitudes. This will allow us to find the magnitude of the meson cloud contribution, and to better specify the N and $P_{11}(1440)$ wave functions.

The results of Refs. [5, 6], where $P_{11}(1440)$ is treated as a hybrid state, are obtained via non relativistic calculations. Nevertheless the suppression of the longitudinal amplitude $S_{1/2}$ has its physical origin in the fact that the longitudinal transition operator for the vertex $\gamma q \rightarrow qG$ requires both spin and angular momentum flip by one unit, while the angular momenta of quarks in the N and $P_{11}(1440) \equiv q^3 G$ are equal to 0. This makes this result

practically independent of relativistic effects. The suppression of the longitudinal amplitude $S_{1/2}$ strongly disagrees with the experimental results.

In summary, for the first time the transverse and longitudinal helicity amplitudes of the $\gamma^* p \rightarrow P_{11}(1440)$ transition are extracted from experimental data at high Q^2 . The results are obtained from differential cross sections and longitudinally polarized beam asymmetry for π^+ electroproduction on protons at $W = 1.15 - 1.69 \text{ GeV}$ [1]. The data were analyzed using two conceptually different approaches, DR and UIM, which give consistent results.

The strong longitudinal coupling rules out the presentation of the Roper resonance as a $q^3 G$ hybrid state, while comparison with quark model predictions provides strong evidence in favor of $P_{11}(1440)$ as a first radial excitation of the $3q$ ground state.

Acknowledgements. The work was supported by U.S. DOE contract DOE/0R/23177-0182.

References

1. K. Park et al., CLAS Collaboration, e-Print Archive: nucl-ex/0709.1946, submitted to Phys. Rev. C.
2. I. G. Aznauryan, V. D. Burkert, H. Egiyan, et al., Phys. Rev. **C71**, 015201 (2005).
3. I. G. Aznauryan, V. D. Burkert, et al., Phys. Rev. **C72**, 045201 (2005).
4. W.-M. Yao et al. [Particle Data Group], J. Phys. **G33**, 1 (2006).
5. Z. Li, Phys. Rev. **D44**, 2841 (1991).
6. Z. Li, V. Burkert, and Z. Li, Phys. Rev. **D46**, 70 (1992).
7. F. Cano and P. González, S. Noguera, B. Desplanques, Nucl. Phys. **A603**, 257 (1996).
8. F. Cano and P. González, Phys. Lett. **B431**, 270 (1998).
9. O. Kreil, C. Hanhart, S. Krewald, and J. Speth, Phys. Rev. **C62**, 025207 (2000).
10. M. Dillig and J. Schott, Phys. Rev. **C75**, 067001 (2007).
11. I. G. Aznauryan, Phys. Rev. **C67**, 015209 (2003).
12. D. Drechsel, O. Hanstein, S. Kamalov, and L. Tiator, Nucl. Phys. **A645**, 145 (1999).
13. R. A. Arndt, W. J. Briscoe, I. I. Strakovsky, and R. L. Workman, Phys. Rev. **C69**, 035213 (2004).
14. R. A. Arndt, W. J. Briscoe, I. I. Strakovsky, and R. L. Workman, Phys. Rev. **C74**, 045205 (2006).
15. R. A. Arndt, W. J. Briscoe, I. I. Strakovsky, and R. L. Workman, Phys. Rev. **C66**, 055213 (2002).
16. V. D. Burkert et al., Phys. Rev. **C67**, 035204 (2003).
17. K. Joo et al., CLAS Collaboration, Phys. Rev. Lett. **88**, 122001 (2002).
18. K. Joo et al., CLAS Collaboration, Phys. Rev. **C68**, 032201 (2003).
19. K. Joo et al., CLAS Collaboration, Phys. Rev. **C70**, 042201 (2004).
20. H. Egiyan et al., CLAS Collaboration, Phys. Rev. **C73**, 025204 (2006).
21. H. J. Weber, Phys. Rev. **C41**, 2783 (1990).
22. S. Capstick and B. D. Keister, Phys. Rev. **D51**, 3598 (1995).
23. F. Cardarelli, E. Pace, G. Salme, and S. Simula, Phys. Lett. **B397**, 13 (1997).

24. B. Juliá-Díaz, D. O. Riska, F. Coester, Phys. Rev. **C69**, 035212 (2004).
25. I. G. Aznauryan, Phys. Rev. **C76**, 025212 (2007).